

NASA TM-81686



3 1176 00166 6487

DOE/NASA/2593-23
NASA TM-81686

NASA-TM-81686 19810018720

Material Response from Mach 0.3 Burner Rig Combustion of a Coal-Oil Mixture

G. J. Santoro, F. D. Calfo,
and F. J. Kohl
National Aeronautics and Space Administration
Lewis Research Center

June 1981

RECEIVED
AUG 15 1981
NATIONAL AERONAUTICS AND SPACE ADMINISTRATION
WASHINGTON, D.C.

Prepared for
U.S. DEPARTMENT OF ENERGY
Fossil Energy
Office of Coal Utilization

NOTICE

This report was prepared to document work sponsored by the United States Government. Neither the United States nor its agent, the United States Department of Energy, nor any Federal employees, nor any of their contractors, subcontractors or their employees, makes any warranty, express or implied, or assumes any legal liability or responsibility for the accuracy, completeness, or usefulness of any information, apparatus, product or process disclosed, or represents that its use would not infringe privately owned rights.

DOE/NASA/2593-23
NASA TM-81686

Material Response from Mach 0.3 Burner Rig Combustion of a Coal-Oil Mixture

G. J. Santoro, F. D. Calfo,
and F. J. Kohl
National Aeronautics and Space Administration
Lewis Research Center
Cleveland, Ohio 44135

June 1981

Work performed for
U.S. DEPARTMENT OF ENERGY.
Fossil Energy
Office of Coal Utilization
Washington, D.C. 20545
Under Interagency Agreement EF-77-A-01-2593

N81-27258 #

MATERIAL RESPONSE FROM MACH 0.3 BURNER RIG COMBUSTION
OF A COAL-OIL MIXTURE

by G. J. Santoro, F. D. Calfo, and F. J. Kohl

National Aeronautics and Space Administration
Lewis Research Center
Cleveland, Ohio 44135

SUMMARY

Wedge-shaped specimens were exposed to the combustion gases of a Mach 0.3 burner rig fueled with a mixture of 40 weight percent micron-size coal particles dispersed in No. 2 fuel oil. Exposure temperature was about 900° C and the test duration was about 44 one-hour cycles. The alloys tested were the nickel-base superalloys, IN-100, U-700 and IN-792, and the cobalt-base superalloy, Mar-M509. The deposits on the specimens were analyzed and the extent of corrosion/erosion was measured. The chemical compositions of the deposits were compared with the predictions from an equilibrium thermodynamic analysis. The experimental results were in very good agreement with the predictions.

INTRODUCTION

The industrial burning of coal-oil mixtures (COM) is a very old idea (ref. 1) which had received renewed interest during World Wars I and II when oil supplies were curtailed and again in 1973 at the start of the oil embargo. At present COM has become one of a number of alternative energy schemes under consideration to reduce this country's dependence on foreign oil (refs. 2 and 3). COM is a mixture of coal particles in oil with the coal in the mixture being as high as 50 weight percent. The fuel mixture has the attraction of stretching the supply of oil while still having the convenience of handling and burning a liquid (refs. 3 and 4). However, from the point of view of air purity standards, COM offers very little advantage over other fuels (ref. 5). Numerous utility boilers in this country originally designed to burn coal have been converted to oil for environmental reasons. These units should be convertible to COM with a minimum of equipment modification. This would offer a relatively "quick-fix" for oil conservation until other more environmentally desirable energy sources become commercially available (refs. 6 to 8).

Most of the attention given to COM has been directed toward its use in utility boilers and blast furnaces (ref. 1). No direct applications of COM in gas turbines have been reported. However, in the past, two programs have examined the direct burning of coal itself to operate a gas turbine. One program was initiated by the Locomotive Development Committee and later continued at the Morgantown Energy Research Center (ref. 9). The second program was conducted in Australia by the Commonwealth Department of National Development and the Joint Coal Board (ref. 10). Both efforts were confronted by the problems of coal handling and preparation; and, worst of all, by the erosivity of coal ash passing through the turbine. By combining very fine coal particles with oil, both the handling and erosivity problems associated with the direct coal method of firing gas turbines should be less severe.

The purpose of this study was to provide an initial evaluation of the response of typical high temperature gas turbine alloys to the combustion gases of COM. The approach taken was to expose test specimens of four superalloy materials to the combustion gases from a modified atmospheric Mach 0.3 burner rig fired by COM. These superalloys are currently being used in turbine blades and vanes. The COM consisted of No. 2 fuel oil with 40 weight percent micron-size coal particles.

Although the burner rig did not simulate all of the parameters of a gas turbine, it was a dynamic gas system and allowed a quick and inexpensive first-cut evaluation of turbine material behavior and the potential of COM for use in gas turbines. The evaluation consisted of observing the ability of the burner to maintain a stable flame and of measuring the deposition and erosion/corrosion occurring on the test specimens. An equilibrium thermodynamic analysis was employed to predict the chemical composition of the deposits, and the calculations were compared with the analyses of the deposits on the test specimens.

EXPERIMENTAL PROCEDURES

Fuel characterization. - Three 55 gallon (208 liters) drums of COM were available for this program. The fuel was supplied by the Department of Energy, Pittsburgh Energy Research Center (PERC). The fuel consisted of 40 weight percent Pittsburgh-seam coal in No. 2 fuel oil with three weight percent lecithin added as a deflocculant. In the as-received fuel the coal particles were at least partially segregated from the oil, forming a thick black sludge on the bottom of the drums. Clearly, continuous mixing of the fuel would be required for firing in the burner rig.

For the purpose of analyzing the fuel, a sample was taken after thorough hand mixing the contents of one of the drums. The chemical analysis and other properties of this fuel are given in table I. The particle size distribution is given in figure 1. The analysis for the major elements and the physical property data were supplied by PERC. The metal content was determined at the Lewis Research Center (LeRC) by a combination of emission and atomic absorption spectrometry. The accuracy of the in-house analyses for metals was estimated to be ± 20 percent of the amount reported for the major metallic elements and ± 50 percent of the amount reported for the trace metals. The major metallic elements present are, of course, the ones which make up the normal mineral content of coal, i.e., silicon, aluminum, iron, calcium, magnesium, sodium, potassium and titanium.

Specimen description. - The composition of the alloys used in this program are listed in table II. The cobalt-base alloy, Mar-M509 is a typical vane material which is generally considered to have good hot corrosion resistance due to its high chromium content. (Hot corrosion is a form of accelerated oxidation (ref. 11) which will be discussed in detail later). The three nickel-base alloys cover a range of hot corrosion resistance. The alloy IN-792 has moderately good hot corrosion resistance, U-700 somewhat poorer, and IN-100 has the least resistance of the four alloys tested (ref. 12).

All the alloys were cast by a commercial vendor into the shape shown in figure 2. All specimens were grit blasted and cleaned with alcohol. Prior to testing, each specimen was measured along a diameter in the center of the expected hottest zone, shown in figure 2, with a bench micrometer to a precision of ± 2 micrometers.

Burner rig operation. - The burner firings were conducted at LeRC Plum Brook Station as part of a larger program employing liquid fuels derived from coal. The test site and the modified Mach 0.3 burner rig have been described previously in detail (ref. 13). In this report we will only summarize the description and include those alterations made to the rig in order to fire the COM fuel.

The fuel drums were located out-of-doors in a diked area about 45 meters from the test cell. The drums were sequentially fitted with a specially prepared lid through which a shaft with attached paddles extended into the drum. The shaft and its paddles were rotated by a pneumatic drill motor attached to the shaft above the drum lid. The drum was pressurized to 3 to 4 psi with service air to provide a head for a high pressure pump which fed the fuel to the test cell through stainless steel tubing. See figure 3 for a fuel mixing and delivery schematic. Along side the COM fuel was a 55 gal drum containing 100 percent No. 2 oil. This fuel was tied into the system upstream of the fuel pump with a valving arrangement which allowed either fuel to be fed into the burner. Prior to each run the system was thoroughly flushed with No. 2 oil to clean the system of any coal sediments from the previous run.

The burner housing of the rig was 28 cm long and about 7 cm in diameter. At one end was attached an exit nozzle and, at the other end, a backplate containing a modified sonic fuel nozzle and the attachments for the fuel and combustion air lines. The burner liner was simply a double opened tube of Inconel-600 that ran from the backplate to the exit nozzle (i.e., no swirl plate or secondary air holes were used.) Some of the combustion air, which was preheated to 370° C, was premixed with the fuel within the sonic fuel nozzle. See figure 4. Combustion was self sustaining after an initial ignition by a spark ignitor located in the burner 3.8 cm downstream of the fuel nozzle. The burner consumed about 4.5 kg of fuel per hour with about 136 kg of air for a fuel-to-air ratio of about 0.03.

A carousel specimen holder accomodating eight wedge-shaped specimens was located downstream of the exit nozzle, figure 5. Two specimens each of IN-792, Mar-M509 and U-700 were placed into the holder. Of the two remaining positions, one was occupied by an IN-100 specimen and the other by a wedge-shaped dummy specimen fitted with a chromel-alumel thermocouple. The carousel was rotated between 300 to 500 rpm about an axis perpendicular to the flame. The temperature of the specimens was adjusted by setting the distance from the exit nozzle because the range of flame temperatures (fuel-to-air ratios) producing a stable burning was severely limited.

Most of the fuel was expended in attempting to modify the rig to improve the burning characteristics. Even the most stable flame achieved was rather poor and the temperature of the specimens during exposure to the combustion gases of this flame varied $\pm 100^{\circ}$ C from the desired temperature of 900° C. When the flame was unstable, friable black coke would build up in the liner of the burner. A typical coke sample was analyzed by x-ray diffraction (XRD) and spectrographically; the results are listed in tables III and IV, respectively. Two types of materials were found, one that was ferromagnetic and one that was not. The elemental content of both types was identical but the composition of the phases was different. The presence of Fe₃O₄ may be responsible for the magnetic property.

Deposition/corrosion procedures. - The superalloy specimens were exposed to the combustion gases of the COM-fueled burner for 44.4 cycles, each cycle consisting of one hour at temperature and 3 minutes of forced air cooling. One hundred cycles were initially anticipated but the fuel was consumed

prior to achieving that goal for reasons explained in the previous section. The deposits on the specimens were analyzed by XRD and spectrographically. Then, cross-sections of the specimens along the plane indicated in figure 2 were metallographically prepared. Measurements were made of the thickness of the alloy visibly unaffected by the corrosion process. These values were subtracted from the original thickness of the specimen and the difference was divided by two. The resultant numbers are defined here as representing the maximum depth of attack.

Thermodynamic analysis and prediction of deposit composition. - The objective of the theoretical analysis was to calculate the composition of gaseous and condensed phase products of COM combustion by taking into account the metal ("mineral") content of the fuel. Previous studies (refs. 13 to 16) have indicated that the condensed phases predicted by a thermodynamic analysis are the ones likely to appear as deposits. Toward this end, the widely used NASA Lewis Complex Chemical Equilibrium Computer Program (CEC) was employed to calculate adiabatic flame temperatures, compositions of combustion gas at any temperature, composition of condensed pure phases (if any form), and thermodynamic dew points for condensation. The CEC program is based on the minimization of free energy approach to chemical equilibrium calculations subject to the constraint of maintaining a proper mass balance between reactants and products. The program permits the calculation of chemical equilibrium composition for homogeneous or heterogeneous systems for assigned thermodynamic states such as temperature-pressure (T,P) and enthalpy-pressure (H,P). For the present work, the role of the major metallic elements in the COM was examined in terms of composition of the gaseous and condensed (solid or liquid) phases as a function of temperature. Most of the thermodynamic data were obtained from the JANAF tables (ref. 18) or the compilation of Barin and Knacke (ref. 19). Note that only those species for which the program was given thermodynamic data were considered in the calculations.

The input parameters for use with the CEC program consisted of the elemental composition of the fuel including the metals Al, Ca, Fe, K, Mg, Na, Si and Ti, as shown in table I. For more details of this procedure see reference 13. The trace elements (concentrations of less than 100 wppm) listed in table I were not included in the thermodynamic analysis because they are not expected to contribute significantly to the composition of the deposits. The gaseous compounds considered by the program include all those listed in table VI of reference 13 and also the gaseous compounds of magnesium: Mg, MgCl, MgCl₂, MgH, MgN, MgO, MgOH, Mg(OH)₂, and MgS. The condensed phase compounds considered in the CEC program are listed in table V of this report.

The condensed phases include a number of the stable minerals expected to form from the combustion of coal (ref. 20), such as mullite (Al₆Si₂O₁₃) and anorthite (CaAl₂Si₂O₈), in addition to a number of other aluminosilicates containing calcium, magnesium, iron, sodium, potassium and titanium. Thermodynamic data for some chemically stable condensed phases were not included in the calculations. These phases were solutions, glasses, or slags which might form from the combination of metals present in the system. Although some of these phases would be expected to appear as stable condensed phases, their inclusion at a future time is not expected to perturb significantly the present results with regard to the composition of gaseous carriers or major condensed elements.

Calculations were performed to simulate the actual conditions of combustion for the COM-fired burner rig deposition/corrosion test. The computer

program was operated in the H,P mode with the initial and final enthalpies equal to that of the reactants at the inlet temperatures in order to calculate the equilibrium adiabatic flame temperature of 1629 K. To arrive at the distribution of molecular species, the program considered simultaneously over 400 gaseous and condensed phase species made up of a minimum of 15 elements.

The calculation of the composition showed that the major gaseous products should be N_2 , O_2 , CO_2 , H_2O , Ar, NO, OH, CO and SO_2 with a large number of CHNOS species in lower concentrations. The metals existed in the gas phase almost exclusively as either metal oxide or hydroxide molecules. At the adiabatic flame temperature, several condensed phases existed in the equilibrium mixture. These are shown in figure 6. The condensed phase of highest concentration was SiO_2 (quartz) with $Al_6Si_2O_{13}$ (mullite), $CaAl_2Si_2O_8$ (anorthite), and Fe_2O_3 (hematite) in lower concentrations. Al_2TiO_5 and $MgSiO_3$ appeared in relatively low concentrations.

In order to aid in the prediction of which compounds would condense on the surface of the specimens, the CEC program was also run in the T,P mode at 25 K temperature intervals from the adiabatic flame temperature down to 900 K. The occurrence of any condensed phases in the calculated compositions was noted. The phases thus identified are also shown in figure 6. The T,P mode calculations showed that there should be an abrupt transformation in the composition of the condensed phases which takes place between 1275 and 1250 K. Below the transformation temperature the major compounds are expected to be $Al_2Si_2O_7$, $CaSiO_3$ (wollastonite), and Fe_2SiO_4 (fayalite). A prediction of the deposit composition can be made from scrutinizing figure 6. The deposit should contain mainly the elements Si, Al, Ca and Fe with much lower amounts of Na, K, Ti and Mg. If the reaction kinetics are sufficiently rapid at 900° C, i.e., deposits can come to equilibrium at the specimen temperature, then the compounds to be expected in the deposit should be those which are stable below the transformation temperature. The deposit then would essentially mirror the mineral/metal content of the fuel. The opposite situation would be the quenching of the high temperature condensed species in the flame without sufficient time during each heat cycle (1 hr) to transform the minerals to their lower temperature phases. In this case those compounds stable above the transformation temperature ought to be the ones found in the deposit.

It is significant that no Na_2SO_4 or K_2SO_4 are predicted to form in the deposits. On this basis, and in conjunction with the fact that no significant levels of vanadium were present in the fuel, classical alkali sulfate- or vanadium-induced hot corrosion would not be predicted. However, large amounts of deposits would be predicted due to the presence of metal oxides.

RESULTS AND DISCUSSION

To properly interpret the results from this study, a few remarks on the diverse nature of coal are required lest specific results be erroneously generalized as applicable to all COM fuels regardless of their source of coal.

Coal can be defined as a heterogeneous sedimentary rock composed principally of macerals (organic constituents) and subordinately of minerals (inorganic constituents) and containing water in submicroscopic pores (ref. 21). The composition of coal varies widely dependent not only on its

geographical origin but also between different coal seams and within individual seams. Coal can be classified by the independent criteria of rank and type. The ranking reflects the stage of metamorphic alteration, from low rank lignite to high rank anthracite, and controls such coal properties as calorific value, hardness, grindability, etc. The type reflects the heterogeneity of coal due to its diverse source and controls the mineral content and ash properties.

Deposit analysis and comparison to predicted composition. - All of the deposits had a reddish color; most were non-adherent and therefore not recovered. Of the deposits remaining on the specimens after the burner rig exposure, those within the maximum temperature zone of each specimen (fig. 2) were examined by XRD. These deposits consisted of a light powdery material that readily came off by a light brushing and a more adherent layer below. There was no indication that the deposits had reacted with the specimens or their oxide scales. In-situ diffraction patterns from the surface of the specimens showed hematite (Fe_2O_3) as the principal phase, table VI. This phase, along with α -quartz (SiO_2) and anorthite ($\text{CaAl}_2\text{Si}_2\text{O}_8$), were components of the deposit, whereas the Cr_2O_3 and spinel were oxidation products of the alloy. The pattern from the loose powder was that of hematite and α -quartz but no anorthite, which apparently had adhered to the surface of the specimens.

The phases detected in the deposits are among those listed in figure 6 above the transformation temperature, i.e., the condensed phases expected to form in the flame provided there is sufficient residence time to establish equilibrium. Of the main species listed (medium to strong) only mullite ($\text{Al}_6\text{Si}_2\text{O}_{13}$) was not detected in the deposit. But mullite was observed in the coke from the liner (table III). It is possible most of this phase was among the unrecovered material that did not adhere to the specimens during their burner rig exposure.

The transformation of coal minerals to ash under simulated pulverized coal firing conditions has been investigated for seven eastern bituminous coals (ref. 20). The phases observed were reported as the ones thermodynamically stable at the combustion temperature. Based on this information and the results of the analysis of the deposits, it appears the original minerals in the coal were transformed to their thermodynamically stable phases at the flame temperature and that these species were then quenched by the specimens. It is also apparent that once quenched (deposited) on the specimens, there was insufficient time at the temperature of the specimens (1 hr per cycle at about 900°C for 44.4 cycles) for these phases to transform to their low temperature forms.

An important point in this analysis is the excellent agreement between the CEC-predicted phases and those actually detected in the deposit. Although the predicted and the detected composition of the deposits were specific for the Pittsburgh-seam coal used in this fuel, the method ought to be valid for CUM fuels prepared with coals from any source. Important to the next section of this report is the prediction that no Na_2SO_4 or K_2SO_4 would form in the deposit.

Corrosion/erosion results. - Photomicrographs of the cross-section of the specimens are given in figure 7. A non-adherent (due to polishing of the mounted specimen) and porous deposit lies over a thin oxide scale. For IN-100, IN-792 and U-700, a zone depleted in the γ' phase, $[\text{Ni}_3(\text{Al},\text{Ti})]$ lies beneath the oxide scale. All four alloys show grain boundary attack just beneath the oxide scale. In table VII the extent of the corrosion is listed in terms of the maximum depth of attack; this region includes the

oxide scale, internal oxidation or grain boundary attack, and any depleted area. The values given in table VII are similar to those obtained in the straight oxidation of these same materials in a Mach 0.3 burner rig fired with Jet A-1 fuel (ref. 22).

Microprobe scans were made of the IN-100 specimen for the chromium and sulfur distribution. The chromium scan is given in figure 8. This alloy is the most susceptible to hot corrosion of the four alloys tested. As seen in figure 8, beneath the porous deposit (25 μm thick) is a thin band enriched in chromium (the Cr_2O_3 scale). Nothing other than background was observed in the sulfur scan. Internal sulfides such as chromium sulfide (CrS) are often identified in materials which have undergone hot corrosion (ref. 11). Hot corrosion occurs in the temperature range from about 750° to 950° C and is believed to be associated with the formation of liquid alkali sulfates. The source of the alkali metal may be either the fuel or the intake air in the case of turbines. The sulfur is present in sufficient quantities in all distillate fuels. The morphology of a hot corroded material often consists of the formation of porous, non-protective scales with an internal layer of sulfides. The extent of the internal sulfide layer can vary from virtually none to a thin band of discrete sulfide particles to a heavy interconnected sulfide area. This description of hot corrosion morphology does not fit that of the specimens here. But the short duration of their exposure in the burner gases may preclude a definite negative assessment because there is evidence for an induction period in hot corrosion during which there is no accelerated attack. However, sulfur has been detected within or below the oxide scales on the nickel-base superalloys B-1900 and NASA-TRW V1A during their induction period (ref. 23) and presumably the same could have occurred with the alloys here if they had been subjected to alkali sulfates in their deposits. Thus, within the exposure limits of the experiment, only straight oxidation probably occurred and this is consistent with the prediction of no alkali sulfate formation.

The well-defined outline of the specimens after their burner rig exposure indicated the absence of erosion. The lack of erosion can be attributed to the small size of the coal particles in the fuel, table I. These micron size coal particles would have been reduced to submicron size ash particles during combustion. Submicron size particles would not have enough inertia to impact on the specimens but they could deposit on the specimens via diffusion through the boundary layer. The latter process could cause corrosion (if it were a reactive deposit) or fouling, but not erosion. The lack of erosion also indicated that the coal particles did not coalesce into substantially larger particles while in the fuel lines or during storage. Thus, the 3 weight percent (with respect to the coal) of liquid lecithin (deflocculant) that had been added to the fuel by the suppliers was effective in preventing the coalescing of the coal particles.

Fouling possibilities. - Fouling is always a potential problem in the utilization of "dirty" fuels such as coals or residual distillates (ref. 24). Fouling in turbines can plug air cooling holes and disrupt efficient aerodynamic flow. The deposits observed on the specimens tested here reached a limited maximum thickness of about 40 μm (figs. 7 and 8) caused at least in part by spallation of some of the deposits by frequent forced air cooling, 3 minutes for every hour at temperature. A utility turbine would not be cycled this frequently and larger deposits might accumulate. The non-adherence of the deposits, however, can also be attributed to their composition. In the direct coal-fired turbine programs (refs. 9 and 10), alkali sulfates were reported to act as bonding agents

causing the other ash particles to agglomerate and to adhere to the turbine blades. This bonding effect was also reported to occur in a turbine simulator fired with actual and synthetic Bunker C fuel (ref. 25). The deposition rate was found to increase with increased concentrations of sodium. The bonding agent was thought to be Na_2SO_4 or one of several low melting Na-V-O compounds. Thus, the predicted absence of alkali sulfates in the deposit and the insignificant level of vanadium in the fuel (table I) not only limited the corrosion but may have contributed to the limited build-up of the deposit.

SUMMARY AND CONCLUDING REMARKS

A COM fuel was fired in a small Mach 0.3 burner rig and typical super-alloys used in turbine airfoils were exposed to the combustion gases at temperatures of about 900°C for about 44 one-hour cycles. The extent of the corrosion was measured and the deposits on the specimens were analyzed. These latter results were compared with predictions from thermodynamic calculations of the combustion products based upon the fuel chemistry, fuel-to-air ratio, and specimen temperature. The composition of the deposits and the absence of hot corrosion attack were accurately predicted. Although these findings are specific for this particular fuel with its particular source and beneficiation of coal, the analysis is generally applicable and indeed had been successfully applied in a previous program involving liquid fuels derived from coal (ref. 13).

REFERENCES

1. Demonstration Program for Coal-Oil Mixture Combustion in an Electric Utility Boiler Category 111A, 1977 Annual Report. HCP/T2564-01, June 1978.
2. Cooper, B. R., ed.: Scientific Problems of Coal Utilization. CONF-770509, 1978.
3. Foster, C. B.: ERDA's Coal-Oil Mixture Combustion Program. ASME Paper 77-WA/Fu-4, Nov. 1977.
4. Campbell, T. C.: Coal-Oil Mixture: Transportation Factors. FE/EES-79/3, 1979.
5. Environmental Readiness Document: Coal-Oil Mixtures. DOE/ERD-0023, 1979.
6. George, T. J.: Economics of Retrofitting Industrial Boilers from Oil to Coal-Oil Mixture Firing. FE/EES-79/4, 1979.
7. LeGassie, R. W. A.: Coal-Oil Mixture - A Fuel for the 80's, 2nd International Symposium on Coal-Oil Mixture Combustion. CONF-791160, Vol. I, 1979, pp. vi-ix. Also see many other related papers in Volume I and Volume II.
8. Session VIII - Economics Regulation and Market Applications, 2nd International Symposium on Coal-Oil Mixture Combustion. CONF-791160, Vol. II, 1979.
9. Smith, J.; et al.: Bureau of Mines Coal-Fired Gas Turbine Research Project. Bureau of Mines Report of Investigation 6920, 1966.
10. The Coal-Burning Gas Turbine Project. Interdepartmental Gas Turbine Project (Canberra, Australia), 1973. AD-914335.
11. Stringer, J.: Hot Corrosion of High Temperature Alloys. Annual Review of Materials Science, Vol. 7, Annual Reviews, Inc., 1977, pp. 477-509.

12. Lowell, C. E.; Sidik, S. M.; and Deadmore, D. L.: Effect of Sodium, Potassium, Magnesium, Calcium, and Chlorine on the High Temperature Corrosion of IN-100, U-700, IN-792 and Mar M-509. DOE/NASA/2593-79/12, NASA TM-79309, 1980.
13. Santoro, G. J.; et al.: "Deposition and Material Response from Mach 0.3 Burner Rig Combustion of SRC-II Fuels," DOE/NASA/2593-80/20, NASA TM-81634, 1980.
14. Kohl, Fred, J.; Stearns, Carl A.; and Fryburg, George, C.: Sodium Sulfate: Vaporization Thermodynamics and Role in Corrosive Flames. Metal-Slag-Gas Reactions and Processes, Z. A. Foroulis and W. W. Smeltzer, eds., The Electrochemical Society, Princeton, NJ, 1975, pp. 649-664; also NASA TM X-71641, 1975.
15. Kohl, F. J.; et al.: Theoretical and Experimental Studies of the Deposition of Na_2SO_4 from Seeded Combustion Gases. J. Electrochem. Soc., vol. 126, no. 6, June 1979, pp. 1054-1061.
16. Miller, R. A.: Analysis of the Response of a Thermal Barrier Coating to Sodium- and Vanadium-Doped Combustion Gases. DOE/NASA/2593-79/7, NASA TM-79205, 1979.
17. Gordon, S.; and McBride, B. J.: Computer Program for Calculation of Complex Chemical Equilibrium Compositions, Rocket Performance, Incident and Reflected Shocks, and Chapman-Jouguet Detonations. NASA SP-273, 1971.
18. Chase, M. W., et al.: JANAF Thermochemical Tables. Dow Chemical Company, Midland, MI, including supplements to June 1978.
19. Barin, I.; and Knacke, O.: Thermochemical Properties of Inorganic Substances. Springer-Verlag, 1973; Barin, I.; Knacke, O.; and Kubaschewski, O.: Thermochemical Properties of Inorganic Substances, Supplement. Springer-Verlag, 1977.
20. Stinespring, C. D.; Zulkoski, M.; and Mazza, M. H.: Chemical Transformation of the Minerals in Eastern Bituminous Coals Under Simulated Pulverized Coal Firing Conditions. Ash Deposits and Corrosion Due to Impurities in Combustion Gases, R. W. Bryers, ed., Hemisphere Publishing Corp., 1978, pp. 233-241.
21. Larsen, J. W.; et al.: Panel Discussion of the Chemical and Physical Characterization of Coal, Scientific Problems of Coal Utilization. CONF-770509, 1978, pp. 76-97.
22. Deadmore, D. L., and Lowell, C. E.: Inhibition of Hot Salt Corrosion by Metallic Additives. DOE/NASA/2593-78/2, NASA TM-78966, 1978.
23. Fryburg, G. C.; Kohl, F. J.; and Stearns, C. A.: Chemical Processes Involved in the Initiation of Hot Corrosion of B-1900 and NASA-TRW VIA. NASA TM-81399, 1979.
24. Reid, W. T.: External Corrosion and Deposits, Boilers and Gas Turbines. American Elsevier Pub. Co., Inc., 1971.
25. Urbas, T. A.; and Tomlinson, L. H.: Part I: Formation and Removal of Residual Fuel Ash Deposits in Gas Turbines Formed at Firing Temperatures Below 982°C (1800°F). Ash Deposits and Corrosion Due to Impurities in Combustion Gases, R. W. Bryers, ed., Hemisphere Pub. Corp., 1978, pp. 309-320.

TABLE I. - COMPOSITION AND PROPERTIES
OF COAL-OIL-MIXTURE FUEL

[40 weight percent Pittsburgh-seam coal
in No. 2 fuel oil.]

Elemental composition (weight percent)			
C	82.5	Al	0.65
H	9.5	Ca	.14
N	0.6	Fe	.35
O	2.8	K	.028
S	0.32	Mg	.024
Cl	.047	Na	.012
		Si	1.9
		Ti	0.042
Ash content (weight percent) 3.7			
Trace metals (wppm)			
Co	5		
Cr	25		
Cu	12		
Mn	40		
Ni	35		
Sr	20		
V	10		
Zr	15		
Heat of combustion, higher heating value (Btu/lb)			17,020
Density (g cm ⁻³)			1.06
Viscosity, at 70° F (centipose)			4000±1000

TABLE II. - ALLOY COMPOSITIONS

[All values are weight percent.]

Alloy				
Element	IN-100	U-700	IN-792	Mar-M509
Cr	10	14.2	12.7	23
Ni	Bal.	Bal.	Bal.	10
Co	15	15.5	9.0	Bal.
Al	5.5	4.2	3.2	-----
Ti	4.7	3.3	4.2	0.2
Mo	3.0	4.4	2.0	-----
W	-----	-----	3.9	7
Ta	-----	-----	3.9	3.5
Nb	-----	-----	0.9	-----
V	1.0	-----	-----	-----
Mn	-----	<0.01	-----	-----
Fe	-----	.1	-----	-----
Si	-----	<.01	-----	-----
Zr	0.6	<.01	0.10	0.5
B	.014	.02	.02	-----
C	.18	.06	.2	0.6

TABLE III. - PHASES DETECTED BY X-RAY DIFFRACTION IN
COKE RECOVERED FROM BURNER LINER

[Listed in order of decreasing line intensities.]

Magnetic material	Non-magnetic material
Fe ₂ O ₃	Spinel ($a_0 = 8.20 \text{ \AA}$)
SiO ₂ (α -quartz)	CaAlSi ₂ O ₈ (anorthite)
CaAl ₂ Si ₂ O ₈ (anorthite)	
Al ₆ Si ₂ O ₁₃ (mullite)	
Fe ₃ O ₄ ($a_0 = 8.30 \text{ \AA}$)	

TABLE IV. - EMISSION SPECTROGRAPHIC ANALYSIS OF
COKE RECOVERED FROM BURNER LINER

[All values are in weight percent.]

Element	Magnetic material	Non-magnetic material
Al	9.8	10.5
Ca	1	1
Cr	<1	<1
Fe	8.4	8.6
Mg	0.1	0.2
Mn	<1	<1
Si	15.0	15.5
Ti	<1	<1
V	<<1	<<1
Na	<3	<3
K	ND ^a	ND

^aND - not determined.

TABLE V. - METAL-CONTAINING CONDENSED PHASES
CONSIDERED IN THE CEC PROGRAM

Metal	Condensed phases
Al	$AlCl_3$, AlN , Al_2O_3 , Al_2S_3 , $Al_2(SO_4)_3$
Ca	$CaCl_2$, $CaCO_3$, CaO , $Ca(OH)_2$, CaS , $CaSO_3$, $CaSO_4$
Fe	$FeCl_2$, $FeCl_3$, FeO , $FeOCl$, Fe_2O_3 , Fe_3O_4 , $Fe(OH)_2$, $Fe(OH)_3$, FeS , FeS_2 , $FeSO_4$, $Fe_2(SO_4)_3$
K	KCN , K_2CO_3 , KO_2 , K_2O , K_2O_2 , KOH , K_2S , K_2SO_3 , K_2SO_4
Mg	$MgCl_2$, $MgCO_3$, MgO , $Mg(OH)_2$, MgS , $MgSO_4$
Na	$NaCl$, $NaCN$, Na_2CO_3 , NaO_2 , Na_2O , Na_2O_2 , $NaOH$, Na_2S , Na_2SO_3 , Na_2SO_4
Si	SiO_2
Ti	TiC , $TiCl_2$, $TiCl_3$, $TiCl_4$, TiN , TiO , TiO_2 , Ti_2O_3 , Ti_3O_5 , Ti_4O_7
	Mixed metal phases
	Al_2SiO_5 , $Al_2Si_2O_7$, Al_2TiO_5 , $Al_6Si_2O_{13}$ $CaAl_2O_4$, $CaAl_2SiO_6$, $CaAl_2Si_2O_8$, $CaAl_4O_7$, $CaFe_2O_4$, $CaMgO_2$, $CaMgSiO_4$, $CaMgSi_2O_6$, $CaSiO_3$, $CaTiO_3$, $CaTiSiO_5$, $Ca_2Al_2SiO_7$, $Ca_2Fe_2O_5$, $Ca_2MgSi_2O_7$, Ca_2SiO_4 , $Ca_3Al_2O_6$, $Ca_3Al_2Si_3O_{12}$, $Ca_3MgSi_2O_8$, Ca_3SiO_5 , Ca_3SiO_5 , $Ca_3Si_2O_7$, $Ca_3Ti_2O_7$, $Ca_4Ti_3O_{10}$ $FeAl_2O_4$, $FeTiO_3$, Fe_2SiO_4

TABLE V. - Concluded.

Mixed metal phases
KAlSi_3O_8 , $\text{K}_2\text{Al}_2\text{Si}_2\text{O}_8$, K_2SiO_3 , $\text{K}_2\text{Si}_4\text{O}_9$ MgAl_2O_4 , MgFe_2O_4 , $\text{Mg}_2\text{Al}_4\text{Si}_5\text{O}_{18}$, MgSiO_3 , MgTiO_3 , MgTi_2O_5 , Mg_2SiO_4 , Mg_2TiO_4 NaAlO_2 , $\text{Na}_2\text{Al}_2\text{Si}_4\text{O}_{12}$, $\text{Na}_2\text{Al}_2\text{Si}_6\text{O}_{16}$, $\text{Na}_2\text{Fe}_2\text{O}_4$, Na_2SiO_3 , $\text{Na}_2\text{Si}_2\text{O}_5$, Na_2TiO_3 , Na_4SiO_4 , $\text{Na}_6\text{Si}_2\text{O}_7$

TABLE VI. - PHASES DETECTED BY X-RAY DIFFRACTION IN
DEPOSITS ON THE SPECIMENS

[Listed in order of decreasing line intensities.
The patterns were essentially the same for de-
posits from all the specimens, except where noted.]

In-situ phases	Phases from loose powder
Fe ₂ O ₃ (hematite)	Fe ₂ O ₃ (hematite)
SiO ₂ (α-quartz)	SiO ₂ (α-quartz)
Cr ₂ O ₃	
CaAl ₂ Si ₂ O ₈ (anorthite)	
Spinel ($a_0 = 8.25 \text{ \AA}$), possibly NiCr ₂ O ₄	
On IN-792 only, a rutile struc- ture, possibly Cr(Ta,Nb)O ₄	

TABLE VII. - CORROSION OF SPECIMENS IN MACH 0.3
BURNER RIG FUELED WITH COAL-OIL MIXTURE

[After 44.4 one-hour cycles at about 900° C.]

Alloy	Maximum depth of attack, μm	Average attack, μm	Depth of attack for 100 h oxidation, μm (ref. 22)
IN-100	78	78	25
U-700	63	68	—
U-700	73		
IN-792	26	22	40
IN-792	18		
Mar-M509	0	5	20
Mar-M509	10		

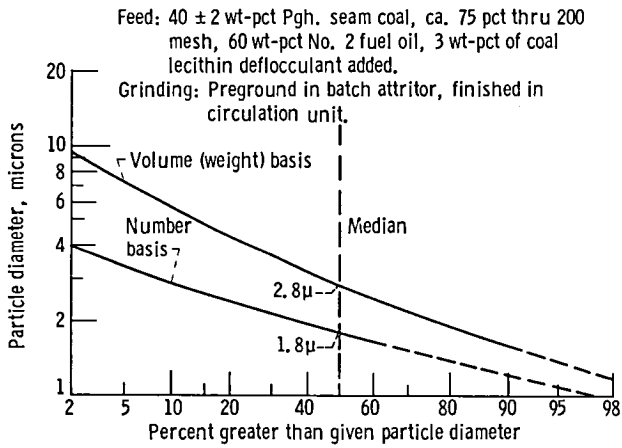


Figure 1. - Particle size distribution of coal particles in coal-oil mixture.

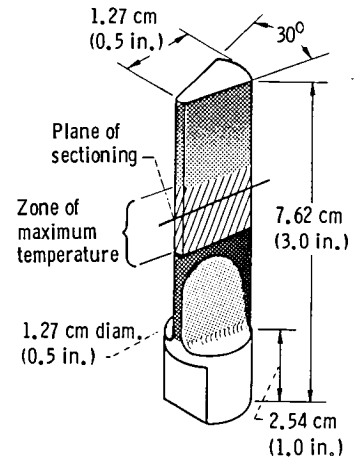


Figure 2. - Test specimen.

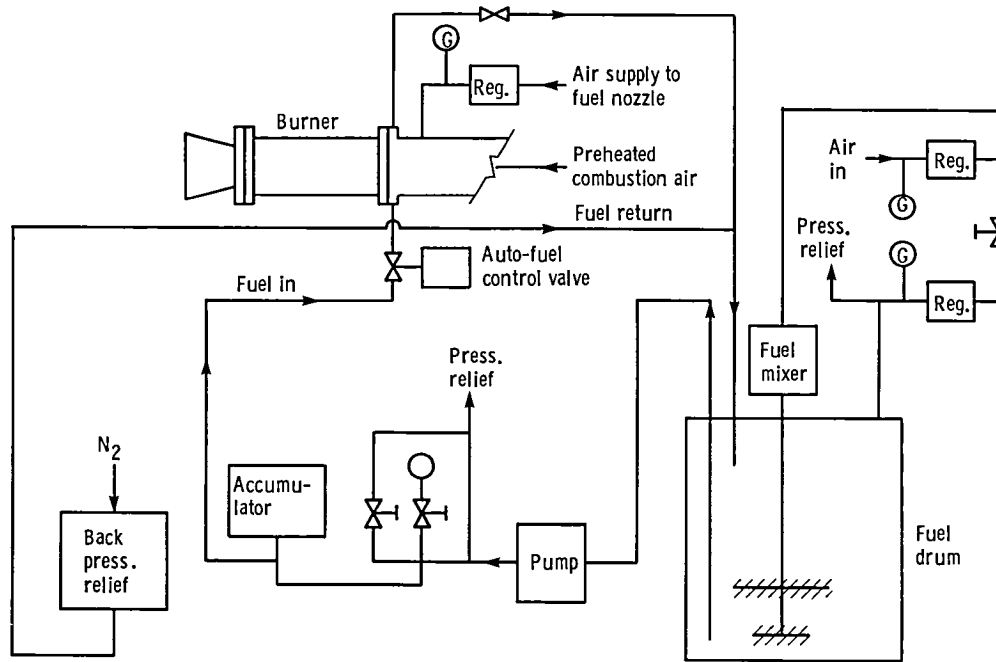


Figure 3. - Fuel mixing and delivery schematic.

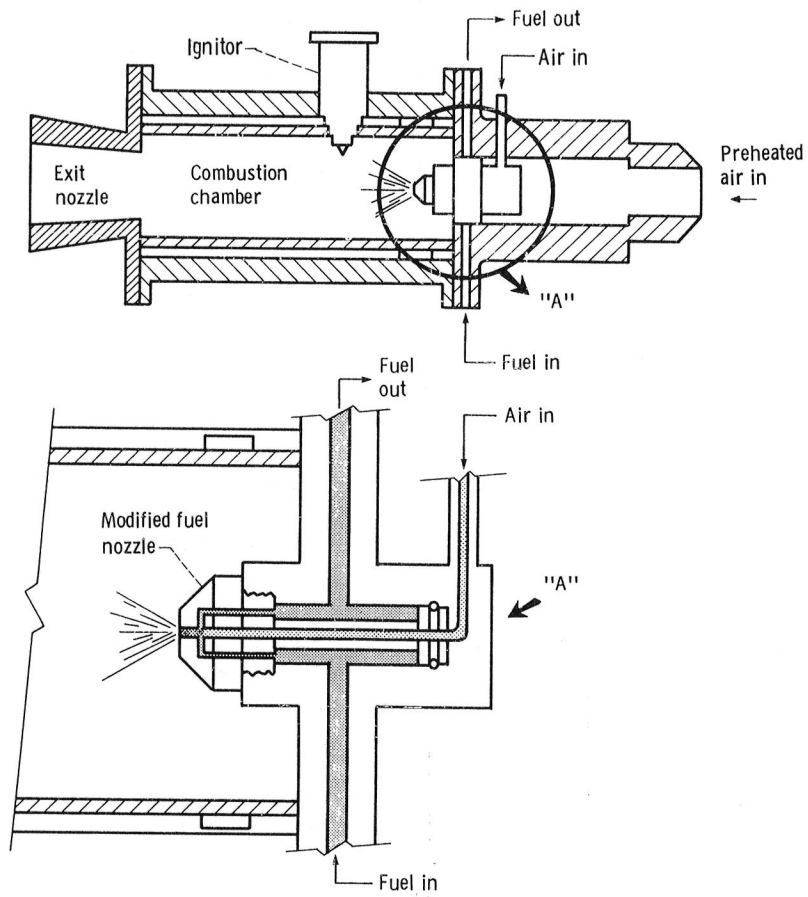


Figure 4. - Modified combustion chamber and fuel nozzle.

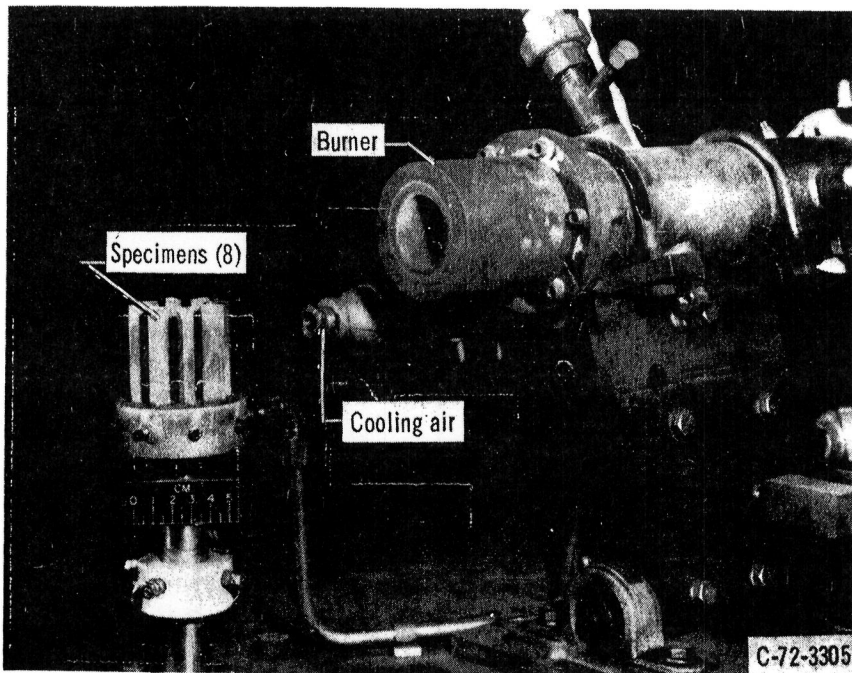


Figure 5. - Burner rig exit nozzle and test specimens

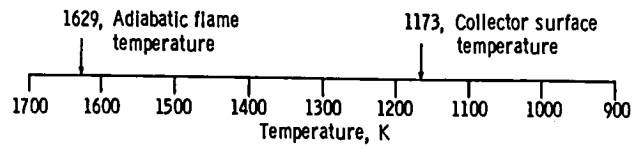
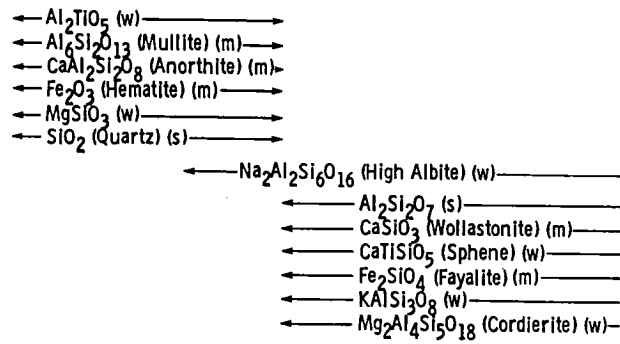
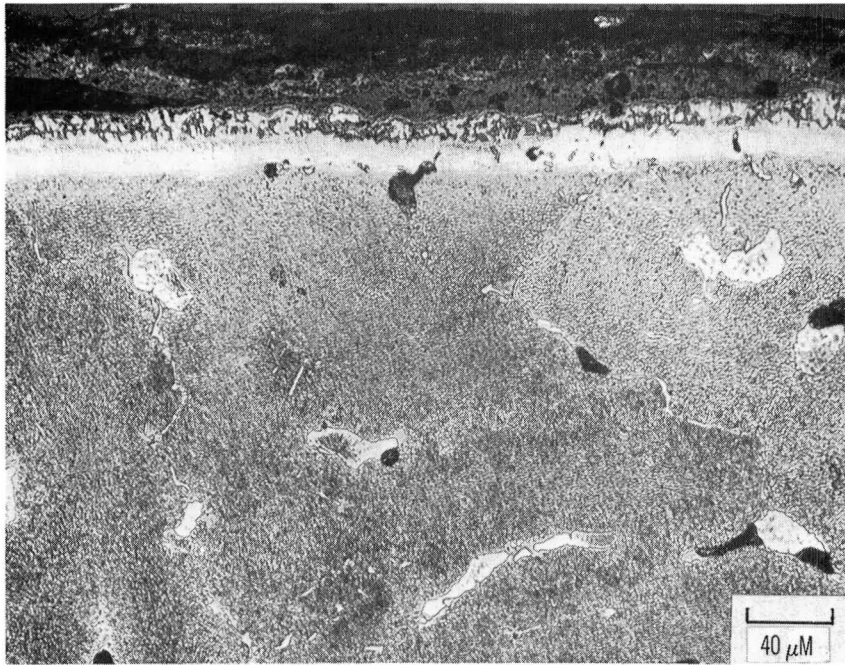


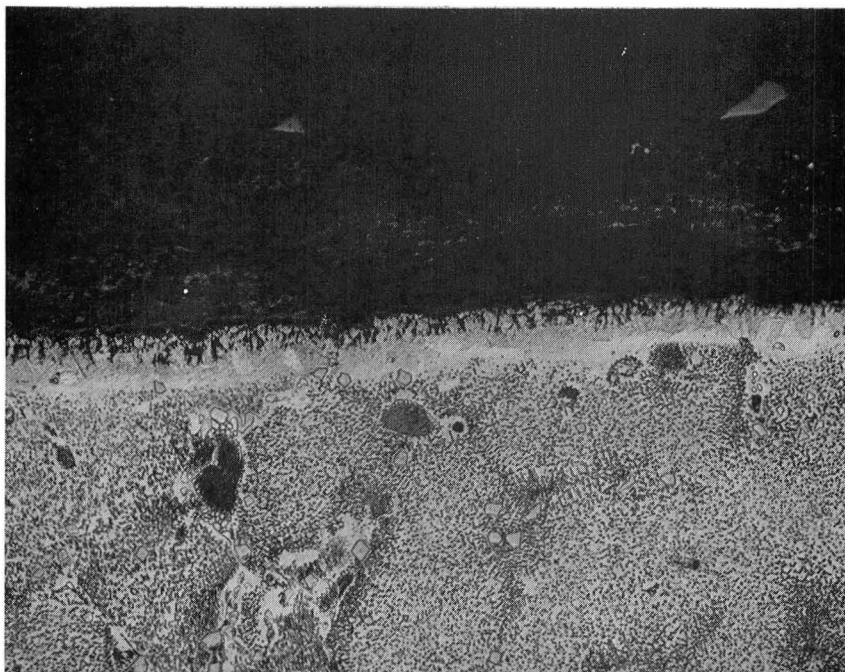
Figure 6. - Equilibrium thermodynamic computer program analysis of condensed phase compositions. Relative concentrations are indicated as strong (s), medium (m), or weak (w).



(a) IN-100.

} Deposit
 } Scale, depleted zone,
 } internal oxidation

Alloy

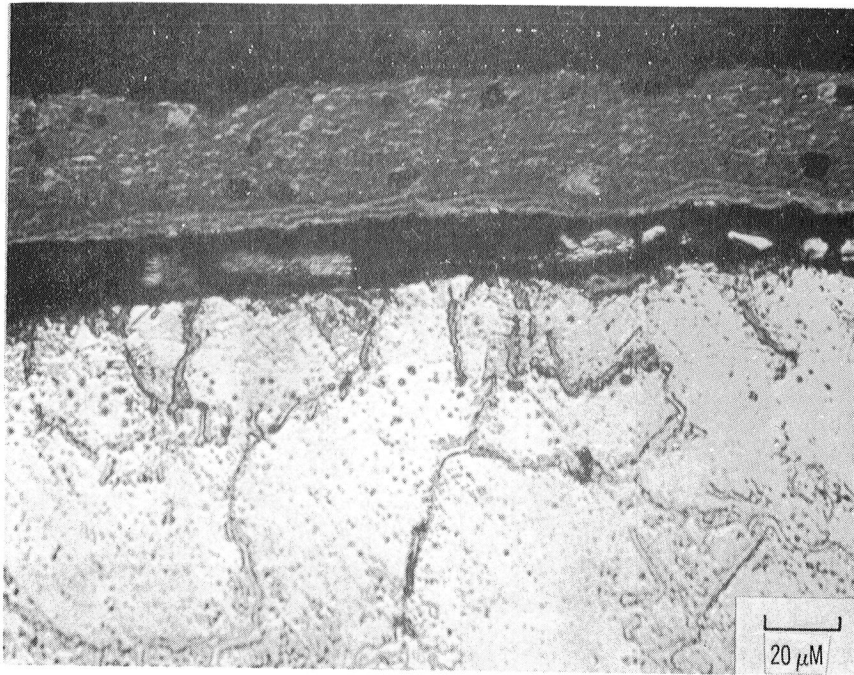


(b) IN-792.

} Deposit
 } Scale, depleted zone,
 } internal oxidation

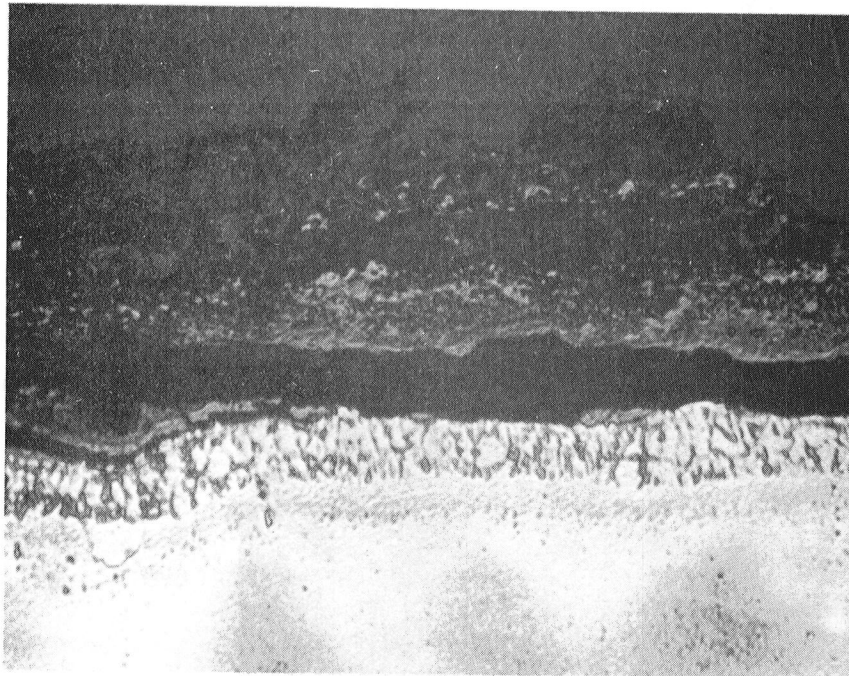
Alloy

Figure 7. - Deposit and corrosion morphology of superalloys exposed in a Mach 0.3 burner rig fueled with coal-oil mixture.



} Deposit
} Scale
} Grain boundary oxidation
Alloy

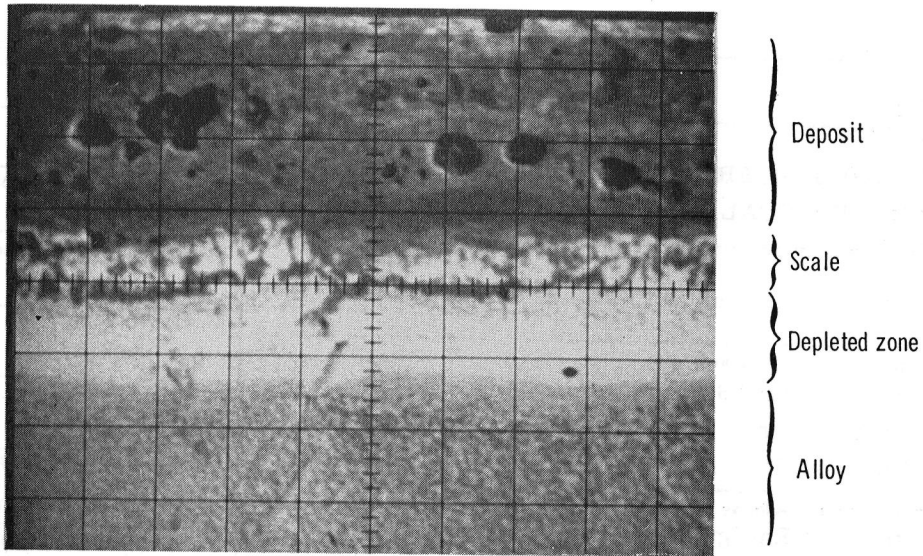
(c) Mar-M509.



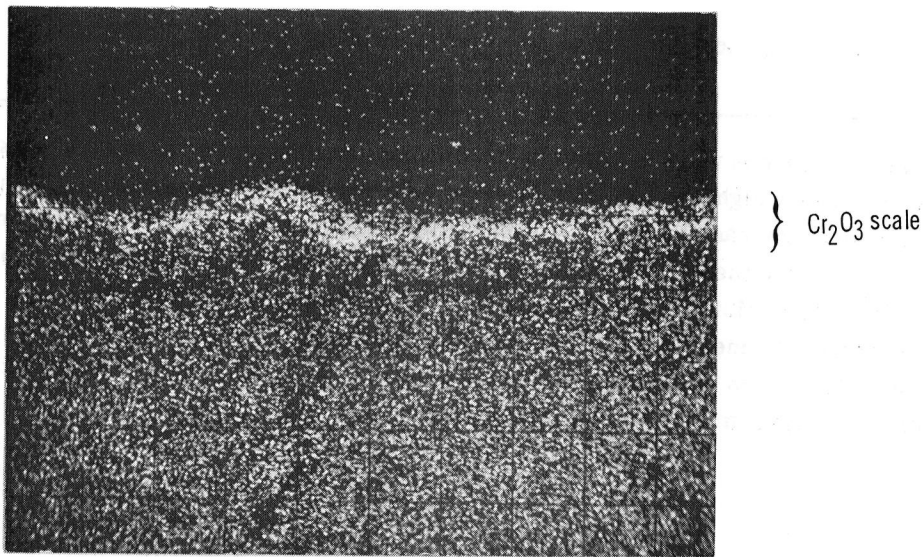
} Deposit
} Scale
} Depleted zone and internal oxidation
Alloy

(d) U-700.

Figure 7. - Concluded.



(a) Secondary electron image.



(b) Chromium K α .

Figure 8. - Raster scans of IN-100 showing (a) deposit, oxide scale and depleted zone and (b) the chromium distribution.

1. Report No. NASA TM-81686	2. Government Accession No.	3. Recipient's Catalog No.	
4. Title and Subtitle MATERIAL RESPONSE FROM MACH 0.3 BURNER RIG COMBUSTION OF A COAL-OIL MIXTURE		5. Report Date June 1981	6. Performing Organization Code 778-11-06
		7. Author(s) G. J. Santoro, F. D. Calfo, and F. J. Kohl	8. Performing Organization Report No. E-718
9. Performing Organization Name and Address National Aeronautics and Space Administration Lewis Research Center Cleveland, Ohio 44135		10. Work Unit No.	
		11. Contract or Grant No.	
12. Sponsoring Agency Name and Address U. S. Department of Energy Office of Coal Utilization Washington, D. C. 20545		13. Type of Report and Period Covered Technical Memorandum	
		14. Sponsoring Agency Code Report No. DOE/NASA/2593-23	
15. Supplementary Notes Prepared under Interagency Agreement EF-77-A-01-2593.			
16. Abstract Wedge-shaped specimens were exposed to the combustion gases of a Mach 0.3 burner rig fueled with a mixture of 40 weight percent micron-size coal particles dispersed in No. 2 fuel oil. Exposure temperature was about 900° C and the test duration was about 44 one-hour cycles. The alloys tested were the nickel-base superalloys, IN-100, U-700 and IN-792, and the cobalt-base superalloy, Mar-M509. The deposits on the specimens were analyzed and the extent of corrosion/erosion was measured. The chemical compositions of the deposits were compared with the predictions from an equilibrium thermodynamic analysis. The experimental results were in very good agreement with the predictions.			
17. Key Words (Suggested by Author(s)) Coal; Fuel combustion; Fuel impurities; Combustion products; Superalloy; Fouling; Chemical equilibrium; Deposition		18. Distribution Statement Unclassified - unlimited STAR Category 26 DOE Category UC-90h	
19. Security Classif. (of this report) Unclassified	20. Security Classif. (of this page) Unclassified	21. No. of Pages	22. Price*

